

# Growth and characterization of excimer laser-ablated $\text{BaBi}_2\text{Nb}_2\text{O}_9$ thin films

A. Laha and S. B Krupanidhi<sup>a)</sup>

Materials Research Centre, Indian Institute of Science, Bangalore-560012, India

The pulsed-laser ablation technique has been employed to deposit polycrystalline thin films of layered-structure ferroelectric  $\text{BaBi}_2\text{Nb}_2\text{O}_9$  (BBN). Low-substrate-temperature growth ( $T_s=400\text{ }^\circ\text{C}$ ) followed by *ex situ* annealing at  $800\text{ }^\circ\text{C}$  for 30 min was performed to obtain a preferred orientation. Ferroelectricity in the films was verified by examining the polarization with the applied electric field and was also confirmed from the capacitance–voltage characteristics. The films exhibited well-defined hysteresis loops, and the values of saturation ( $P_s$ ) and remanent ( $P_r$ ) polarization were 4.0 and  $1.2\text{ }\mu\text{C}/\text{cm}^2$ , respectively. The room-temperature dielectric constant and dissipation factor were 214 and 0.04, respectively, at a frequency of 100 kHz. A phase transition from a ferroelectric to paraelectric state of the BBN thin film was observed at  $220\text{ }^\circ\text{C}$ . The dissipation factor of the film was observed to increase after the phase transition due to a probable influence of dc conduction at high temperatures. The real and imaginary part of the dielectric constant also exhibited strong frequency dispersion at high temperatures.

Presently, ferroelectric thin films are recognized as promising candidates for generation data storage devices, such as nonvolatile random access memories (NVRAMs).<sup>1</sup> Extensive work has been done on  $\text{PrZr}_x\text{Ti}_{1-x}\text{O}_3$  (PZT) for the development of NVRAMs due to its nonvolatility, large remanent polarization ( $P_r$ ), fast switching speed, and radiation hardness. However, one of the most serious damages associated with Pt/PZT/Pt ferroelectric capacitors is the degradation of the polarization hysteresis characteristics. To avoid such fatigue problems with PZT thin films, Bi-layered compounds have been used for better fatigue properties. These layered perovskites belong to the Aurivillius family,<sup>2,3</sup> with a general formula  $(\text{Bi}_2\text{O}_2)^{2+}(\text{A}_{n-1}\text{B}_n\text{O}_{3n-1})^{2-}$ . The layered-structure compounds<sup>4</sup> meet the requirements for NVRAMs without showing any significant fatigue even after  $10^{11}$ – $10^{12}$  switching cycles.<sup>5–7</sup> Among these materials,  $\text{SrBi}_2\text{Ta}_2\text{O}_9$  (SBT),  $\text{SrBi}_2\text{Nb}_2\text{O}_9$  (SBN), their solid solutions, and other similar compounds, have been widely studied.<sup>8–10</sup>

In this letter, we report the growth and characterization of polycrystalline  $\text{BaBi}_2\text{Nb}_2\text{O}_9$  (BBN) thin films. BBN is another member of the Aurivillius family, and the study of dielectric and electric properties of BBN thin films is thus of interest.<sup>11</sup> Platinum-coated silicon substrates were used to deposit the BBN thin films by pulsed-laser ablation technique using a single-phase target prepared by the conventional ceramic route with 10% excess of  $\text{Bi}_2\text{O}_3$ . The calcination and sintering conditions of the target were 800 and  $1050\text{ }^\circ\text{C}$  for 90 min, respectively. The films were grown by a Lambda Physik (KrF) excimer laser ( $\lambda=248\text{ nm}$ ) at a frequency of 5 Hz and an energy fluence of  $4\text{ J}/\text{cm}^2$ . The distance between the target and the substrate was maintained at 30 mm. Prior to the deposition process the base pressure was brought down to  $2.2\times 10^{-5}$  Torr. The oxygen pressure and substrate temperature during deposition were maintained at

250 mTorr and  $400\text{ }^\circ\text{C}$ , respectively. A relatively high oxygen pressure was used to maintain compatibility between the number of oxygen molecules impinging on the substrate surface per unit time in this range of pressure and ablated ions/atoms arriving from the target per second. The as-deposited films were annealed at  $800\text{ }^\circ\text{C}$  for 30 min in a quartz-tube furnace under flowing oxygen. The crystallographic structure of the film and the target were confirmed by x-ray diffraction (XRD) using  $\text{Cu K}\alpha$  radiation. A semiquantitative analysis of the film composition was performed by energy-dispersive analysis of x rays (EDAX). Gold top electrodes of a thickness of  $100\text{ \AA}$  were deposited at room temperature by a thermal evaporation process through a shadow mask of the area  $1.96\times 10^{-3}\text{ cm}^2$ . The thickness of the film was confirmed using an optical spectrometer (Filmetrics F-20 thin-film measurement system), which measures thin-film characteristics by either reflecting or transmitting light through the sample, and then analyzing this light over a range of wavelengths. Polarization hysteresis behavior was studied using a RT-66A standardized ferroelectric test system in virtual ground mode. The variation of capacitance with the external dc electric field was studied using an automated Keithley 3330 LCZ meter in conjunction with a Keithley source measure unit (model 236) in a frequency range of 0.1–100 KHz over a temperature range of 30–300 °C.

The x-ray diffraction patterns of a conventionally annealed BBN thin film and the target are shown in Fig. 1. The as-deposited films ( $T_s=400\text{ }^\circ\text{C}$ ) were found to be amorphous and the crystallization process was completed after annealing at  $800\text{ }^\circ\text{C}$  for 30 min. The x-ray diffraction pattern of the film matches that of the target quite well. The grain size in the film, calculated from the Scherrer equation, was found to be 35–45 nm. From the compositional analysis (obtained by EDAX) of the film annealed at  $800\text{ }^\circ\text{C}/30\text{ min}$ , the atomic ratio of Ba:Bi:Nb was found to be 1:2.5:2, indicating the presence of a slight bismuth excess. The presence of excess Bi is desirable as it helps to bring down the crystallization

<sup>a)</sup>Author to whom correspondence should be addressed; electronic mail: [sbk@mrc.iisc.ernet.in](mailto:sbk@mrc.iisc.ernet.in)

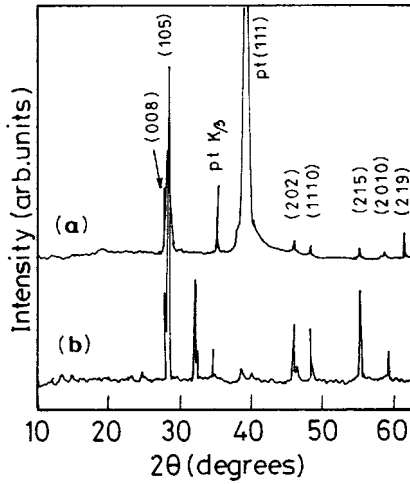


FIG. 1. X-ray diffraction patterns of (a) BBN thin film annealed at 800 °C for 30 min; (b) BBN target sintered at 1050 °C for 90 min.

temperature. However, too much excess Bi was observed to degrade the properties of the film as a consequence of  $\text{Bi}_2\text{O}_3$  segregation from the rest of the matrix.<sup>12</sup>

The ferroelectric nature of the BBN thin films was confirmed from the polarization hysteresis measurements, as shown in Fig. 2. The measured values of the spontaneous and remanent polarization were 4.0 and 1.2  $\mu\text{C}/\text{cm}^2$ , respectively, with a coercive field of 60 kV/cm. The capacitance–voltage ( $C$ – $V$ ) characteristics of a BBN thin film are shown in Fig. 3 at two different frequencies, 10 and 100 kHz, respectively. By applying a small ac signal of 50 mV amplitude with a varying dc electric field following the sequence of negative  $\Rightarrow$  positive  $\Rightarrow$  negative bias direction, the  $C$ – $V$  measurements were carried out. The butterfly shape of the curve confirmed the ferroelectric nature of the film. The two maxima of the loop correspond to domain-switching voltages in forward and reverse directions where the polarization reversal takes place. The slight asymmetry in the  $C$ – $V$  curve may be due to different electrode/ferroelectric interfaces.

Figures 4(a) and 4(b) represent the frequency dispersion of the real ( $\epsilon'_r$ ) and imaginary ( $\epsilon''_r$ ) part of the dielectric constant, respectively. At lower frequencies (100 Hz) the value of  $\epsilon'_r$  increases sharply with temperature, whereas at higher frequencies the dependence of  $\epsilon'_r$  on temperature comes down. The severe low-frequency dependence of  $\epsilon'_r$  on

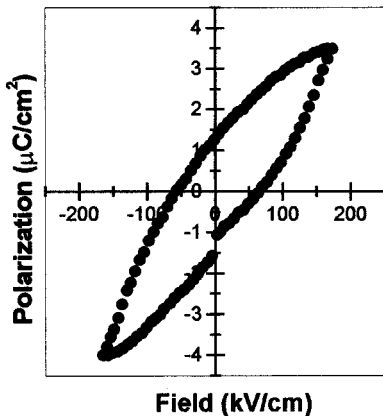


FIG. 2. Polarization-field hysteresis behavior of a BBN thin film.

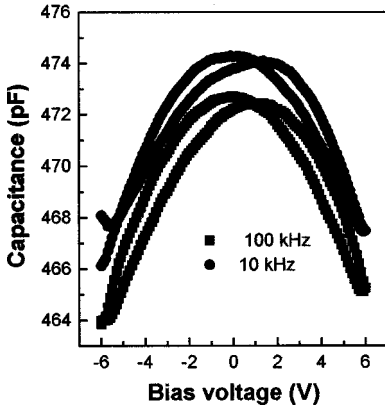


FIG. 3. Capacitance–voltage characteristics of a BBN thin film.

temperature indicates the contribution of the space charge to the complex dielectric constant, whereas at higher frequencies the merging of the dielectric dispersion curves at all measured temperatures suggests that the space-charge effect diminishes gradually.<sup>13</sup> The influence of space charge is also reflected in the imaginary part of the dielectric constant ( $\epsilon''_r$ ), where we observe similar frequency dispersion at higher temperature. More studies are in progress in terms of orientation effects on the ferroelectric behavior and associated charge-transport mechanisms.

The variation of dielectric constant ( $\epsilon'_r$ ), as well as dissipation factor ( $\tan \delta$ ) with temperature, are shown in Fig. 5.

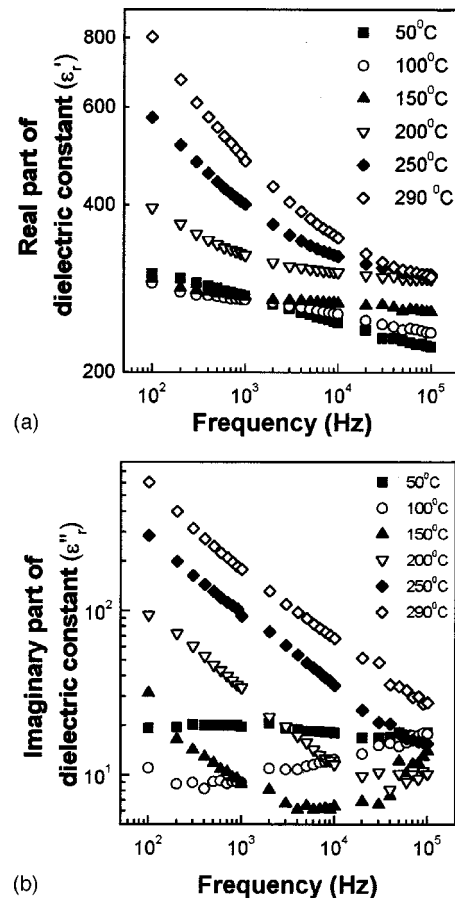


FIG. 4. (a) Frequency dispersion of the real part of the dielectric constant ( $\epsilon'_r$ ) for different temperatures. (b) Imaginary part of the dielectric constant ( $\epsilon''_r$ ) plotted as a function of frequency for different temperatures.

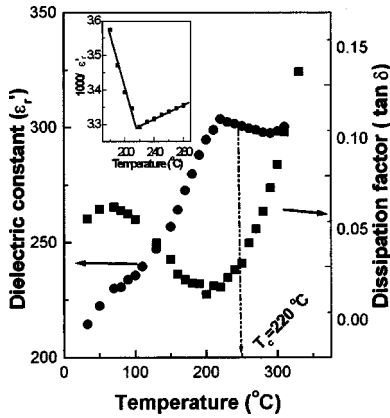


FIG. 5. Relative dielectric constant ( $\epsilon''$ ) and dissipation factor ( $\tan \delta$ ) as a function of temperature. The inset shows the  $1000/\epsilon''$  vs temperature plot.

The room-temperature dielectric constant ( $\epsilon''$ ) was 214 with  $\tan \delta$  of 0.04 at a frequency of 100 kHz. The value of  $\epsilon''$  increased with temperature and reached a maximum value of 304 at  $220^\circ\text{C}$  ( $T_c$ ) and showed a decreasing trend above  $T_c$ , which is the characteristic property of a ferroelectric material. The slightly higher value of  $T_c$  of the BBN thin film, compared to the reported value of bulk ceramics ( $T_c = 200^\circ\text{C}$ ),<sup>4</sup> could be due to the residual stress developed at grain boundaries, as well as at the film–substrate interface and associated space charges. The BBN thin films tend to exhibit a second-order phase transition at  $T_c$ , which was confirmed from the temperature dependence of the reciprocal dielectric constant on both sides of the transition temperature, as shown in the inset of Fig. 5. It can be noted that the slope in the ferroelectric region differs in magnitude and sign from that in the paraelectric region. The dissipation factor was observed to increase at higher temperatures, which could be attributed to an enhanced dc charge leakage property at elevated temperatures.

In conclusion, polycrystalline thin films of layered-structure ferroelectric  $\text{BaBi}_2\text{Nb}_2\text{O}_9$  were deposited using the pulsed-laser ablation technique. A low substrate temperature during deposition and a subsequent annealing were applied to obtain the polycrystalline thin films, which are desirable to

obtain good ferroelectric properties. The films exhibited a room-temperature dielectric constant of about 214 with a dissipation factor of 0.04 at a frequency of 100 kHz. The ferroelectric behavior was confirmed both from polarization hysteresis and capacitance–voltage measurements. The measured values of remanent and saturation polarization were 1.2 and  $4.0 \mu\text{C}/\text{cm}^2$ , respectively, with a coercive field of 60 kV/cm. The impact of the space-charge contribution to the real and imaginary part of the dielectric constant was clearly observed from the low-frequency dispersion of  $\epsilon'_r$  and  $\epsilon''_r$ . The ferroelectric phase transition of BBN films showed a slightly diffuse nature, and the measured value of the transition temperature was about  $220^\circ\text{C}$ , which was slightly higher than that reported for bulk ceramics. From the nature of the ferroelectric transition, it is anticipated that the films exhibit a second-order phase transition.

The authors would like to acknowledge the Department of Science and Technology, India, and the Indian Space Research Organization (ISRO) for the financial assistance to carry out the present work.

- <sup>1</sup>J. F. Scott and C. A. Paz de Araujo, *Science* **246**, 1400 (1989).
- <sup>2</sup>B. Aurivillius, *Ark. Kemi* **2**, 519 (1950).
- <sup>3</sup>B. Aurivillius and P. H. Fang, *Phys. Rev.* **126**, 893 (1962).
- <sup>4</sup>E. C. Subbarao, *J. Phys. Chem. Solids* **23**, 665 (1962).
- <sup>5</sup>J. F. Scott, M. C. Scott, C. A. Paz de Araujo, J. D. Cuchiaro, and L. D. McMillan, *Nature (London)* **374**, 627 (1995).
- <sup>6</sup>K. Amanuma, T. Hase, and Y. Miyasaka, *Appl. Phys. Lett.* **66**, 221 (1995).
- <sup>7</sup>C. A. Paz de Araujo, J. D. Cuchiaro, L. D. McMillan, M. C. Scott, and J. F. Scott, *Nature (London)* **374**, 627 (1995).
- <sup>8</sup>R. Dat, J. K. Lee, O. Auciello, and A. I. Kingon, *Appl. Phys. Lett.* **67**, 572 (1995).
- <sup>9</sup>S. Bhattacharyya, S. S. N. Bharadwaja, and S. B. Krupanidhi, *Appl. Phys. Lett.* **75**, 2656 (1999).
- <sup>10</sup>K. M. Satyalakshmi, M. Alexe, A. Pignolet, N. D. Zakharov, C. Harnagea, S. Senz, and D. Hesse, *Appl. Phys. Lett.* **74**, 603 (1999).
- <sup>11</sup>J. S. Morrell, Z. B. Xue, E. D. Specht, and D. B. Beach, *Mater. Res. Soc. Symp. Proc.*, 271 (1998).
- <sup>12</sup>M. A. Rodriguez, T. Boyle, A. Hernandez, C. D. Buchheit, and M. O. Eatough, *J. Mater. Res.* **11**, 2282 (1996).
- <sup>13</sup>S. Saha and S. B. Krupanidhi, in *Proceedings of the 12th International Symposium on Integrated Ferroelectrics*, Aachen, Germany (March, 2000) (unpublished).